Optimization of the square and squared-off cascades to separate stable isotopes using meta-heuristic algorithms

Fatemeh Ardestani · Jaber Safdari · Mohammad Hassan Mallah · Morteza Imani

Received: 7 January 2022 / Accepted: 15 August 2022 / Published online: 9 April 2024

Abstract
In this paper, the optimization of the square and squared-off cascades for the separation of stable isotopes with a certain number of gas centrifuges (GCs) using particle swarm optimization (PSO) and the whale optimization algorithm (WOA) was studied. For this purpose, the "SC-PSO" and "SC-WOA" codes for the square cascade (SC), and the "SOC-PSO" and "SOC-WOA" codes for the squared-off cascade (SOC) were developed. The performance of the PSO and WOA algorithms in the optimization of the square and squared-off cascades as an example for the separation of ^{124}Xe from nine stable isotopes of xenon up to an enrichment of 85% was compared. The recovery coefficient of ^{124}Xe isotope by the codes "SC-PSO", "SC-WOA", "SOC-PSO", and "SOC-WOA" was obtained 86.14, 78.11, 92.84, and 83.41% respectively. The performance of the algorithms indicates the higher yield of the PSO algorithm in the optimization of SC and SOC. The efficiency of the PSO has been demonstrated by the Griewank test function compared with the WOA, the sine cosine algorithm (SCA), and the dragon-fly algorithm (DA) (PSO>WOA>SCA>DA). Furthermore, the results show that SOC performs better than SC.

Keywords Square cascade · Squared-off cascade · Gas centrifuge · Particle swarm optimization algorithm · Whale optimization algorithm · Multicomponent separation

Introduction

Today, owing to the need for isotopic products, research on the production processes and applications of stable isotopes is of particular importance. Many elements in nature have several isotopes with different properties. Stable isotopes are classified into industrial, medical (diagnosis and treatment), agricultural, and research-based isotopes [1]. The element xenon has nine stable isotopes that are used in various industries. ^{124}Xe is mainly used in medicine such as produce of ^{123}I radioisotope in the diagnosis of a variety of diseases. Also, ^{122}I and ^{125}I radioisotopes are produced using ^{124}Xe. In addition, xenon isotopes such as ^{126}Xe are used in the production of ^{128}Ba radioisotope for diagnostic imaging. It is worth mentioning that ^{130}Xe, ^{134}Xe, and ^{138}Xe are utilized in nuclear physic research. Owing to the widespread applications of stable isotopes in various industries, their enrichment is essential [2, 3]. The concentration of ^{124}Xe in natural feed is very low (0.09%); therefore, it requires several stages of enrichment to reach high concentrations [2]. The separation of stable isotopes by gas centrifuge (GC) is performed by cascades of centrifuges. In a general category, cascades can be classified into three types: tapered, square, and squared-off. In a tapered cascade, the feed flow rate into stages changes continuously from stage to stage. As a result, the size of the stages and the number of centrifuges in each stage change by the same process [4, 5]. In a square cascade (SC), the feed flow rate into stages is equal; therefore,

used at low feed flow rates and different cuts. These types of cascades have great flexibility in operation. Thus, SCs are the most suitable cascades for separating stable isotopes. Stable isotopes are very diverse and the ways of separating them are all different [4]. Tapered cascades are notable for their high separation efficiency and SCs are important for their great flexibility. If a tapered cascade includes a set of the SCs connected in a series, this type of cascade is named a *squared-off cascade* (SOC). The performance of SOCs is between the tapered and square cascades. Multi-section SOCs can be two-section, three-section, and so on. In each section, the feed flow rate into stages is equal to each other; also, the number of GCs is the same in each stage.

Several research projects on the modeling and numerical simulation of square and squared-off cascades have been reported so far. SC modeling for the separation of multicomponent isotopes was studied in 1994 [6]. Separation of ^{116}Cd isotope was investigated using SC numerical simulation up to 95% enrichment [7]. Governing equations for a multicomponent isotope separation SC were presented by Kholpanov et al. in 1998 [8]. Borisevich et al. investigated the separation of cadmium isotopes using SC simulations [9]. They also studied the separation of molybdenum isotopes by SC and SOC and used a genetic algorithm to optimize the cascades [10]. Mansourzadeh et al. used tapered and square cascades by the teaching learning-based optimization (TLBO) algorithm to separate ^{129}Xe isotope with up to 91.2% enrichment [11]. The separation of silicon and cadmium isotopes was investigated using optimization of an SC by Azizov et al. [12]. In the present research, for the first time, the simulation and optimization of SC and two-section SOC for the separation of all stable multicomponent isotopes are done using particle swarm optimization (PSO) and the whale optimization algorithm (WOA). SC had two return flows at the beginning and at the end of the cascade and the two-section SOC had three return flows at the beginning, at the end, and between the two sections. Therefore, it was necessary to add two parameters ($\theta_{Cascade}$, θ_1) and three parameters ($\theta_{Cascade}$, θ_1, λ) to the input parameters of both cascades respectively. To this end, the number of equations and unknown parameters were equalized to each other, which made the simulation possible. In the optimization process, a random number between zero and one is generated for each parameter. This random number is multiplied by the upper and lower bounds of each optimization parameter that is given as input to the code, and finally, this number is rounded for parameters that are integer such as N_F.

The purpose of optimizing the parameters is to maximize the amount of product with specific concentration, recovery factor, and D parameter. Owing to the limited separative power of GC, it is not possible to achieve a certain enrichment of the target isotope in one step. Thus, it is necessary to use several separation steps.

The present study, to our knowledge for the first time, presents the optimal square and squared-off cascades using PSO and the WOA to separate all stable multicomponent isotopes. For this purpose, the "SC-PSO," "SC-WOA," "SOC-PSO," and the "SOC-WOA" codes have been developed to optimize the parameters of SC and SOC. In the present work, the two-section SOC is investigated. The square and two-section squared-off optimization codes are able to optimize the parameters of N_F, F, L_s, θ_1, $\theta_{Cascade}$, and λ (SOC) to achieve the desired enrichment of the target isotope. In order to select the best SC as an example of the enrichment of ^{124}Xe using 160 GCs, all possible cascades are examined by "SC-PSO." Finally, the best SC with the highest recovery factor and the largest amount of product is selected. Also the types of two-section SOC arrangements with the number of stages appropriate to the selected SC, where the feed enters the first or second section, are studied by "SOC-PSO." In this research, appropriate solutions to increase the enrichment of ^{124}Xe to a specific concentration are prepared using SC and two-section SOC. In addition, the performance of the "SC-PSO" and "SC-WOA" codes in optimizing SC and the performance of the "SOC-PSO" and "SOC-WOA" codes in optimizing the two-section SOC are compared. Finally, the best SC and SOC for ^{124}Xe enrichment are compared based on their performance.

Simulation and optimization

Modeling of SC and two-section SOC

In an SC, the feed flow rate into stages is constant; hence, the number of GCs in each stage is the same. In two-section SOCs, the cascade is divided into two sections; in each section, the feed flow rate is constant, and therefore, the number of GCs in each section is similar. Figure 1a,b illustrates a schematic of SC and a two-section SOC. N represents the total number of stages in the cascade and n indicates the number of stages. According to Fig. 1a,b, the stages' feed stream in SCs is constant and shown by L. The stages' feed stream into two sections of SOCs is shown with L_1 and L_2 respectively [8]. The two-section SOCs are classified into two types depending on whether the feed enters the first or the second section. If the cascade feed enters the first section, the value of L_1 is greater than L_2 and vice versa. The exiting light and heavy streams from the cascade stages are indicated by L'_n and L''_n respectively.

Also, the concentration of the desired isotope (i) in the stages' feed, light and heavy streams are shown by $C_{i,n}$, $C'_{i,n}$ and $C''_{i,n}$ respectively. N_c is the number of elements in the mixture of various multicomponents. The index i corresponds to the i component, which can have values between 1 and N_c (i = 1, 2, ..., N_c). The cascade receives a mixture of feed (F) with C_i^F composition and generates a product stream (P or L) with $C'_{i,p}$ composition and a waste stream (W or H) with $C''_{i,w}$ composition. The return flows ε_1, $\varepsilon_{\acute{N}}$ (in SC and SOC) and λ (in the two-section SOCs) are used in the initial and final stages and between the two sections to keep the feed flow rate into the stages constant [8].

The purpose of numerically simulating and solving the equations of a cascade is to determine the values of its unknown parameters. All the unknown parameters of SC and two-section SOC are presented in Table 1. In order to determine the unknown parameters, it is necessary to specify the equations governing the cascades. Tables 2 and 3 present the governing equations of SC and two-section SOC respectively. As can be seen, total numbers of SC and two-section SOC equations are less than the total number of their corresponding unknown

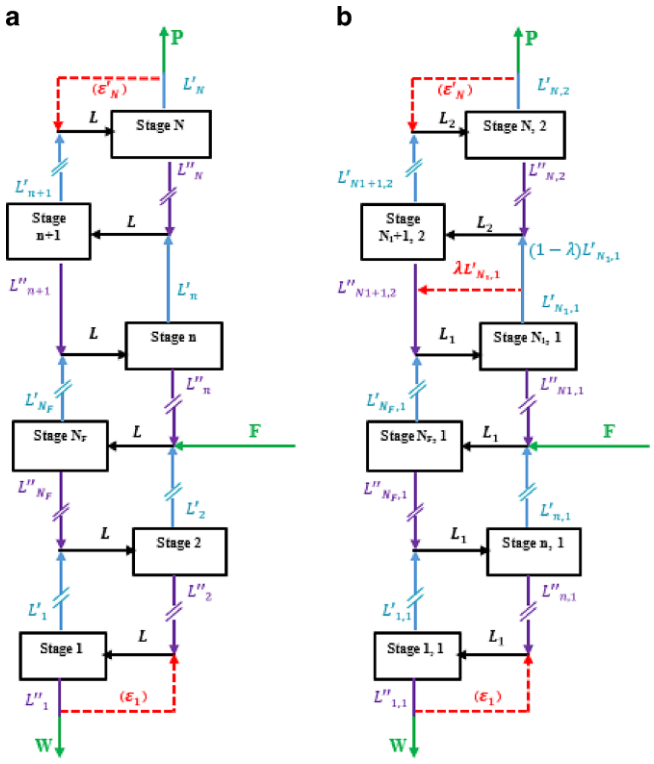

Fig. 1 Scheme of separating cascades (**a**) SC (**b**) two-section SOC with N stages [5, 8]

Table 1 Unknown Parameters of SC and Two-Section SOC [8, 11]

Unknown parameters related to concentration		Unknown parameters related to flow rate	
Sign	Number	Sign	Number
$C_{i,n}$	NN_c	L'_n	N
$C'_{i,n}$	NN_c	L''_n	N
$C''_{i,n}$	NN_c	θ_n	N
Total unknowns related to the concentration of SCs	$3NN_c$	P	*1*
Total unknowns related to the concentration of two-section SOCs	$3NN_c$	W	*1*
–	–	θ_{Cascade}	*1*
–		ε_1	*1*
		$\varepsilon\prime_N$	*1*
		λ	*1*
		Total unknowns related to the flow rate of SCs	*3N+5*
		Total unknowns related to the concentration of two-section SOCs	*3N+6*
Total number of unknown parameters of SCs		$(3N_c+3)N+5$	
Total number of unknown parameters of two-section SOCs		$(3N_c+3)N+6$	

Table 2 Governing Equations of SCs [11, 13–15]

Equations related to flow rate	Number	Equations related to concentration	Number
$L_n - L\prime_n - L\prime\prime_n = 0$	N	$L_n C_{i,n} - L''_n C''_{i,n} - L'_n C'_{i,n} = 0$	$N(N_c-1)$
$L_1 - L''_2 - \varepsilon - \delta(1, N_F)\, Feed = 0$	N	$L_1 C_{i,1} - L''_2 C''_{i,2} - \varepsilon C''_{i,W} - \delta(1, N_F)\, F C^F_{i,1} = 0$	$N(N_c-1)$
$L_n - L\prime_{n-1} - L\prime\prime_{n+1} - \delta(n, \text{NF})F = 0$		$L''_{n+1} C''_{i,n+1} + L'_{n-1} C'_{i,n-1} + \delta(n, \text{NF}) F C^F_{i,n} - L_n C_{i,n} = 0$	
$L_N - L'_{N-1} - \varepsilon\prime - \delta(N, N_F)\, F = 0$		$L_N C_{i,N} - L'_{N-1} C'_{i,N-1} - \varepsilon\prime C'_{i,P} - \delta(N, N_F)\, F C^F_{i,N} = 0$	
$L\prime_n = L_n \theta_n$	N	$\alpha_{ik,n} = \frac{C'_{i,n}}{C''_{i,n}} / \frac{C'_{k,n}}{C''_{k,n}} = \alpha_0^{M_k - M_i}$	$N(N_c-1)$
$P = F\theta_{\text{Cascade}}$	1	$\sum_i C_{i,n} = \sum_i C'_{i,n} = \sum_i C''_{i,n} = 1$	$3N$
$P + \varepsilon\prime = L\prime_N$	1	–	
$W + \varepsilon = L\prime\prime_1$	1		
Total equations		$(3N_c+3)N+3$	

parameters. Therefore, by assuming the values of this number of unknown parameters, cascade simulation will be possible. It is clear that the assumed values for these parameters will affect the values of other parameters as well. In cascade optimization, the values of these parameters are optimized according to the purpose of the optimization. For modeling and solving the equations of SC and two-section SOC, at first, the equations related to the intermediate flow rates are solved and then the intermediate flow concentrations are calculated. This leads to a set of linear equations in the form of a matrix, AX = B, which can be solved numerically by this matrix. The concentration distribution along the cascade can be determined using the q iteration method [13].

It should be noted that in the above tables, the Kronecker function δ is defined as follows:

$$\delta = \begin{cases} 1 & n = N_F \\ 0 & n \neq N_F \end{cases} \tag{1}$$

In this research, the PSO and WOA were used to optimize the SC and two-section SOC parameters.

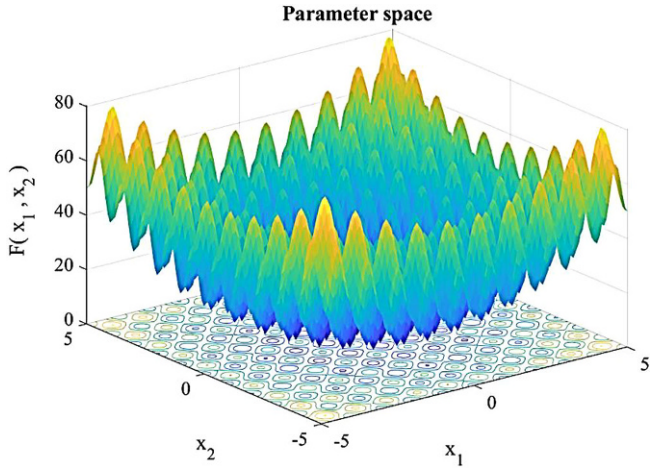

Fig. 2 Griewank test function

Evaluation of the PSO and WOA algorithms

The choice of the PSO algorithm is due to proving the power and efficiency of this algorithm in optimizing cascades by other researchers [3, 16, 17]. There are many meta-heuristic algorithms, but owing to a large number of these algorithms, the WOA, the SCA, and dragon-fly algorithm (DA) were selected because of their high citations. To specify the efficiency of the algorithms, the PSO, WOA, SCA, and DA algorithms have been checked in the Griewank function. This is a unimodal and continuous function that can be defined in n-dimensional space [18]:

$$f\ (x) = f\ (x_1, \ldots, x_n) = 1 + \sum_{i=1}^{n} \frac{x^2}{4000} - \prod_{i=1}^{n} \cos\left(\frac{x}{\sqrt{i}}\right) \tag{2}$$

In this research, the value of n is considered 2 (Fig. 2). This function is usually appraised on $-600 \le x_i \le 600$ for ($i = 1, 2, \ldots, n$). The absolute minimum is $f(x) = 0$, at $x = (0, 0 \ldots, 0)$.

The values presented in Table 4 show that PSO has the best fitness value of 0.10627, which effectively minimizes the Griewank function after PSO, WOA, SCA, and DA have indicated great execution respectively. It appears that PSO is a powerful optimization strategy that can give predominant results to the Griewank function. Owing to the close efficiency of WOA to PSO, the performance of both algorithms in cascade optimization has been investigated.

PSO algorithm

The PSO algorithm operates based on the random production of the initial population. In this algorithm, each particle has a specific velocity. These particles move in the search space at a speed that is dynamically adjusted according to their previous behavior. As a result, they tend to go to the best and most appropriate search area during the search phase. This algorithm has been taken based on simulating the social behavior of a group of birds in finding food. Each bird leaves its flow location depending on its previous location or contact with one of the group members who has found the best food. The algorithm starts by selecting a population of particles in the search space that are assigned to each particle's location, velocity, and fit value in the objective function [19]. All particles know their best location, the best location of the group members, and also the value of the objective function in the locations. The behavior of a particle in the PSO algorithm can be divided into three categories: (1) continuing its motion in the direction of the path it has taken, (2) moving toward the best

Table 3 Governing Equations of Two-Section SOCs [8, 13, 15]

Equations related to flow rate	Number	Equations related to concentration	Number
$L_n - L\prime_n - L\prime\prime_n = 0\ 1 \le n \le N$	N	$C_{i,n}L_s - C\prime_{i,n}L\prime_{n,s} - C\prime\prime_{i,n}L\prime\prime_{n,s} = 0\ 1 \le n \le N$	$N(N_c - 1)$
$L_1 - L''_{2,1} - \varepsilon_1 - \delta\,(1, N_F)\,F = 0$	N	$C_{i,1}L_1 - C''_{i,2}L''_2 - C''_{i,W}\varepsilon - \delta\,(1, N_F)\,FC^F_{i,1} = 0$	$N(N_c - 1)$
$L_1 - L''_{n+1,1} - L'_{n-1,1} - \delta\,(n, N_F)\,F = 0$		$C_{i,n}L_1 - C\prime_{i,n-1}L\prime_{n-1,1} - C\prime\prime_{i,n+1}L\prime\prime_{n+1,1} - \delta\,(n, N_F)\,FC^F_{i,n} = 0$	
$L_1 - L''_{N1+1,,2} - L\prime_{N1-1,1} - \lambda L\prime_{N1,1} - \delta\,(N_1, N_F)\,F = 0$		$C_{i,N1}L_1 - C\prime\prime_{i,,N1+1}L''_{N1+1,,2} - C\prime_{i,N1-1}L\prime_{N1-1,1} - \lambda C\prime_{i,N1}L\prime_{N1,1} - \delta\,(N_1, N_F)\,FC^F_{i,N1} = 0$	
$L_2 - L''_{N1+1,2} - (1-\lambda)L\prime_{N1-1,1} - \delta\,(N_1 + 1, N_F)\,F = 0$		$C_{i,N_1+1}L_2 - C''_{i,N_1+2}L''_{N_1+2,2} - C\prime_{i,N_1}(1-\lambda)\,L'_{N_1,1} - \delta\,(N_1 + 1, N_F)\,FC^F_{i,N1+1} = 0$	
$L_2 - L''_{n+1,2} - L'_{n-1,2} - \delta\,(n, N_F)\,F = 0$		$C_{i,n}L_2 - C''_{i,n+1}L''_{n+1,2} - C\prime_{i,n-1}L'_{n-1,2} - \delta\,(n, N_F)\,FC^F_{i,n} = 0$	
$L_2 - L'_{N-1,2} - \varepsilon\prime_N - \delta\,(N, N_F)\,F = 0$		$C_{i,N}L_2 - C'_{i,N-1}L'_{N-1,2} - C\prime_{i,P}\varepsilon\prime - \delta\,(N, N_F)\,FC^F_{i,N} = 0$	
$L\prime_n = L_n\theta_n$	N	$\frac{C\prime_{i,n}/C\prime_{j,n}}{C\prime\prime_{i,n}/C\prime\prime_{i,n}} = \alpha_{0,n}^{M_j - M_i}\ (i = j-1, j = 2, \ldots, N_c)$	$N(N_c - 1)$
$P = F\theta_{\text{Cascade}}$	1		
$L\prime\prime_{1,1} - W - \varepsilon_1 = 0$	1	$\sum_{i=1}^{N_c} C_{i,n} = \sum_{i=1}^{N_c} C\prime_{i,n} = \sum_{i=1}^{N_c} C\prime\prime_{i,n} = 1$	$3N$
$L\prime_{N,2} - \varepsilon\prime_N - P = 0$	1	–	
Total equations		$(3N_c + 3)\,N + 3$	

Table 4 The Best Fitness Values for Griewank Function by the PSO, WOA, SCA, and DA

Run No	PSO		WOA		SCA		DA	
Best results	Iteration	Fitness	Iteration	Fitness	Iteration	Fitness	Iteration	Fitness
1	100	0.33505	100	0.27033	100	1.04672	100	2.24425
2	200	0.13786	200	0.17586	200	0.46163	200	2.01428
3	500	0.12662	500	0.16585	500	0.22622	500	0.67122
4	800	0.10874	800	0.15419	800	0.19459	800	0.73443
5	1000	0.10627	1000	0.14734	1000	0.17681	1000	0.61262
Average	–	0.16291	–	0.18271	–	0.42119	–	1.25536

position it has taken, and (3) moving toward the best position found by the whole group (whole particles). The mathematical expression describing the above motion is according to the following relations:

$$V^i\,[\mathrm{t}+1] = \mathrm{w}V^i\,[\mathrm{t}] + C_1 r_1\left(x^{i,\text{best}} - x^i[t]\right) + C_2 r_2\left(x^{\text{Global best}} - x^i[t]\right) \tag{3}$$

$$x^i\,[\mathrm{t}+1] = x^i\,[t] + V^i\,[\mathrm{t}+1] \tag{4}$$

The coefficients *w, C_1*, and C_2 indicate the degree of confidence of the particle in its flow location, in its previous experience, and in its adjacent particles respectively [19]. In other words, *w, C_1* and C_2 are named *the coefficients of inertia, individual learning* and *collective learning* with the following values respectively:

$$0.4 \le \mathrm{w} \le 0.9$$

$$0 \le C_1 \le 2$$

$$0 \le C_2 \le 2.$$

These coefficients are usually randomly selected at each optimization step. In fact, in this method, each particle in the search space moves at a speed proportional to the best previous location of that particle and the

best place among all the particles. Each particle's location indicates a current (temporary) candidate answer to the optimization problem. Specifically, the parameters used in Eqs. 2 and 3 are as follows: $V^i\,[t]$ = velocity of a particle in each stage, x^i = particle's location in each stage, (r_1 and r_2) = random numbers between zero and one, t = time, and i = current optimization stage number. In fact, the above two commands are the same rules of self-optimization in the PSO algorithm, and all particles have to execute them. Whenever the particle achieves a new position, it should be checked whether or not it has hit its record; if yes, it should be checked whether or not it has hit the aggregate record. In fact, for each new particle position, the best particle record (i, Best) and the best particle total record (Global Best) must be updated. For the PSO algorithm, the following general stages can be mentioned:

1. creating the initial population and evaluating them,
2. determining the best personal memory and the best collective memory,
3. updating the speed and position and evaluating new responses, and
4. if the stop conditions are not met, go to stage 2; otherwise,
5. End.

WOA algorithm

Humpback whales are able to identify the location of the prey and surround it. As the optimal design location in the search space is unknown, the WOA algorithm assumes that the current best solution candidate is pre-target or near-optimal prey. Once the best search factor is defined, other factors try to change their location to the best factor. This behavior is shown by Eqs. 4 and 5 [20]:

$$\vec{D} = \left|\vec{C}.\vec{X^*}(t) - \vec{X}(t)\right| \tag{5}$$

$$\vec{X}(t+1) = \vec{X^*}(t) - \vec{A}.\vec{D}. \tag{6}$$

Where, t represents current iterations, $\vec{A}$ and $\vec{C}$ indicate coefficient vectors, $\vec{X^*}$ shows the vector of the best current solution's position and $\vec{X}$ is the vector of the position. It is worth mentioning that in each iteration of the algorithm, if there is a better answer, X^* must be updated. Vectors $\vec{A}$ and $\vec{C}$ are obtained using the following equations [20]:

$$\vec{A} = 2\vec{a}\,\vec{r} - \vec{a} \tag{7}$$

$$\vec{C} = 2\vec{r}, \tag{8}$$

where, the value of $\vec{a}$ decreases linearly from 2 to 0 during the iterations (both in the detection and the colonization phases) and $\vec{r}$ is the random vector at a distance of [0, 1]. Figure 3a illustrates the logic behind Eq. 5 for a 2-D problem. Position (X, Y) is a search agent that can be updated according to the best current position (X^*, Y^*). Different areas around the best factor can be obtained according to the current position by adjusting the value of vectors $\vec{A}$ and $\vec{C}$ Fig. 3b also displays the possible modified position for a 3-D search agent. It is to be noted that by defining a random vector $\vec{r}$, it would be possible to achieve any position in the search space located between the key points. Hence, Eq. 6 paves the way for each search agent to change its position in the area to the best current solution, and thus, simulate prey siege [20].

Whales attack the prey with a bubble-net search mechanism. To model the bubble behavior of whales, two mechanisms have been designed: *spiral updating position* and *shrinkage encircling mechanism*. The spiral updating position first calculates the distance between the whale in place (X, Y) and the prey in place (X^*, Y^*).

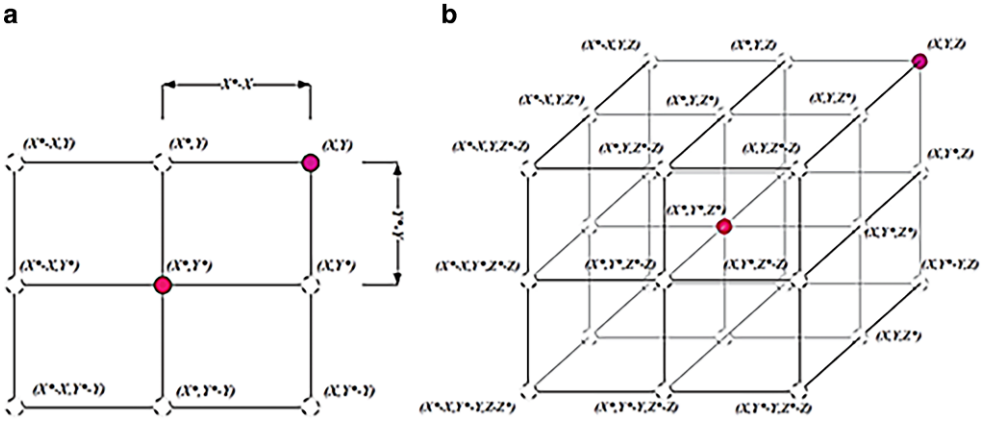

Fig. 3 **a** Two-dimensional and (**b**) three-dimensional location vectors and their next possible location in the WOA algorithm [20]

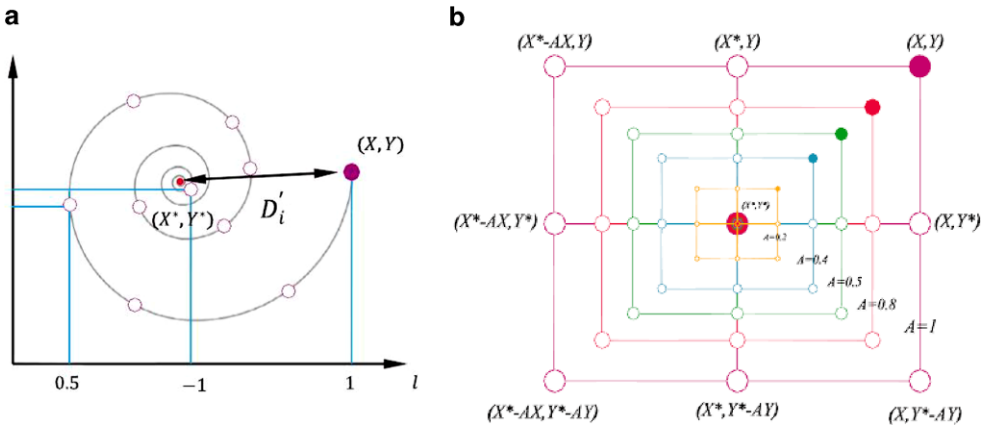

Fig. 4 Bubble-net (colonial phase) search mechanism implemented in WOA. **a** Spiral updating position and (**b**) shrinking encircling mechanism [20]

Then a spiral equation is created between the location of the whale and the prey to represent the circular motion of the whale (Fig. 4a):

$$\vec{X}(t+1) = \vec{D}e^{bl}Cos(2\pi l) + \vec{X^*}(t), \tag{9}$$

where, $\vec{D} = \left|\vec{X^*}(t)\right| - \vec{X}$, and indicates the distance between the ith whale of the prey, b is a constant for defining the shape of a logarithmic spiral, and l is a random number in the range [–1, 1]. The shrinkage encircling mechanism is based on the amount of reduction of $\vec{a}$ in Eq. 7. In other words, $\vec{A}$ is a random value between [–a, a] where $\vec{a}$ decreases from 2 to 0 during the iterations. By placing the random value of $\vec{A}$ in the range [–1, 1], the new location of a search agent can be anywhere between its original location and the location of the best current agent. Figure 4b shows the possible locations from (*X, Y*) to (X^*, Y^*) that are obtained according to $0 \le A \le 1$ in the 2-D space [20].

It should be mentioned that whales swim around the prey in a shrinking circle and a spiral path. To model these two simultaneous movements, it is assumed that, with a 50% probability, a shrinking siege mechanism or spiral model will be selected to update the location of the whales during optimization as below:

$$\overrightarrow{X}(t+1) = \begin{cases} \overrightarrow{X^*}(t) - \overrightarrow{A}.\overrightarrow{D} & if \;\; p < 0.5 \\ \overrightarrow{D} e^{bl} Cos(2\pi l) + \overrightarrow{X^*}(t) & if \;\; p \geq 0.5 \end{cases}, \tag{10}$$

where, p is a random number within the range [0, 1]. This algorithm is able to change between the spiral and circular motions based on the value of p. It is worth noting that WOA includes only two main internal parameters (A, C) that need to be adjusted [20].

Objective functions

In this study, the purpose of optimization is to increase the enrichment of ^{124}Xe isotope up to 85% and achieve the maximum value of the final product. The objective functions are given in Eq. 11. According to this equation, the cascade parameters are optimized in such a way that the maximum recovery coefficient, cascade capacity, and two-group parameter (D) are obtained in each separation step to achieve the maximum amount of product with a concentration of 85%.

$$\text{Objective Function} = \begin{cases} \min\left(C_1 \frac{W}{\mathrm{F}} + C_2 (1 - R_{\text{calc}}) + C_3 (1 - D) + C_4 \left| C_{i,\text{calc}} - C_i^P \right|\right) & \text{if target in light Stream} \\ \min\left(C_1 \frac{P}{\mathrm{F}} + C_2 (1 - R_{\text{calc}}) + C_3 (1 - D) + C_4 \left| C_{i,\text{calc}} - C_i^W \right|\right) & \text{if target in heavy Stream} \end{cases} \tag{11}$$

where, C_i represents the value of the final concentration, calc index shows the values calculated from the simulation, R is the cascade's recovery coefficient, C_i^P indicates the optimal value of concentration in light flow, C_i^W represents the desired value of concentration in heavy flow, and C_1, C_2, C_3, and C_4 (having constant values) represent the weights of each of the objective functions. The value of each of the expressions in the objective function (Eq. 11) is numerically between zero and one. The term of min (W/F) is used to reduce as much as possible the amount of waste, and to increase the amount of consumed feed in the cascade (if the target is in a light stream). Therefore, owing to the existence of several separation steps, maximizing the feed capacity of the cascade in a certain period of time is one of the important purposes of optimization.

The second expression in the objective function is related to the cascade's recovery coefficient. It is clear that a higher recovery coefficient means greater efficiency of the cascade. The cascade's recovery coefficient is calculated as below:

$$\begin{aligned} R &= \frac{P C_i^P}{F C_i^F} \quad \text{if target in light Stream} \\ R &= \frac{W C_i^W}{F C_i^F} \quad \text{if target in heavy Stream.} \end{aligned} \tag{12}$$

The third expression in the objective function is related to the two-group parameter (D). The D parameter is mainly used as a criterion for the separation of two isotopic groups from multi-component mixtures. In other words, this parameter is a good criterion for determining the accuracy of the separation path with several steps. Increasing the D parameter leads to the separation of the target isotope from other isotopes [15]. Accordingly, when the two groups of light and heavy are separated partially or completely, the value of the D function will always be $D \leq 1.0$. Isotopes of a multicomponent element are divided into the light and heavy groups according to their molecular weight. It is worth noting that the target isotope can be placed in both groups. Research has shown that isotope (k) is the lightest component if it falls in the heavy group, and it is the heaviest component

if it falls in the light group [13]. Depending on the target isotope's position (light or heavy stream), we use Eq. 13 or 14:

$$D = \frac{P}{F}\sum_{i=1}^{k} C'_{i,N} + \frac{W}{F}\sum_{i=k+1}^{N_c} C''_{i,1} \text{ k in the light stream} \tag{13}$$

$$D = \frac{P}{F}\sum_{i=1}^{k-1} C'_{i,N} + \frac{W}{F}\sum_{i=k}^{N_c} C''_{i,1} \text{ k in the heavy stream} \tag{14}$$

Determining the position of the target isotope in the group of light or heavy isotopes plays a key role in achieving the maximum enrichment of isotope in the final product. As a result, the cascade parameters are optimized in such a way that the D parameter is maximized. In other words, specification of the target isotope's position in the group of light or heavy isotopes is also called determining the separation path. The separation path determines which of the light or heavy products output from the cascade as the desired product. For this purpose, the maximum target isotope enrichment in the light and heavy streams is calculated by Eqs. 15 and 16.

$$C'_{\max,k} = \frac{C_{F,k}}{\sum_{i=1}^{k} C_{F,i}} \tag{15}$$

$$C''_{\max,k} = \frac{C_{F,k}}{\sum_{i=k}^{N_c} C_{F,i}}. \tag{16}$$

The separation path is determined based on the maximum enrichment of the target isotopes in the streams (Eqs. 15 and 16). If the optimal product with the desired enrichment is not achieved in the first step, this product is used as a cascade feed in the next step and the separation path is determined accordingly.

Finally, the fourth expression is $\left|C_{i,\text{calc}} - C_i^P\right|$. This expression is applied as a design constraint in code optimization. In this way, the desired richness (C_i^P) is given as a code input and the purpose is to minimize the above expression. The optimization algorithm for the SC and SOC to achieve the desired enrichment of the target isotope is presented in Fig. 5.

Results and discussion

Comparison of the results of the suggested code with those of other researchers

To confirm the validity of the suggested codes, the results are compared with the values presented by Azizov et al. [12]. They utilized the ABC algorithm for SC optimization [12]. Furthermore, the results are compared with other optimization algorithms such as WOA, SCA, PSO, and DA. Based on this reference, the α_0 and the cascade product flow rate are considered $\sqrt{3}$ and 1 g/s [12]. The isotope studied in this comparison is ^{28}Si and its purpose is to increase its richness to 99.99% in the light stream and decrease to 0.01% in the heavy stream. The natural concentration of silicon isotopes (^{28}Si, ^{29}Si, and ^{30}Si) in the feed are 92.21%, 4.7%, and 3.09%. The total flow rates ($\sum L$) obtained by the ABC, WOA, SCA, DA, and PSO algorithms are about 291.31, 368.08, 550.16, 400.76, and 276.12 g/s respectively (Table 5). Also, the values of the C_{si-28}^P, C_{si-28}^W, N, and N_F in the corresponding optimized cascades are shown in Table 5.

The results indicate that PSO reached the optimal parameters of the cascade with a better fitness value in comparison with the WOA, SCA, and DA. Owing to the good results of SC-PSO, the PSO can be utilized as an appropriate method for designing SC. Figure 6 shows less iteration for convergence by the PSO algorithm.

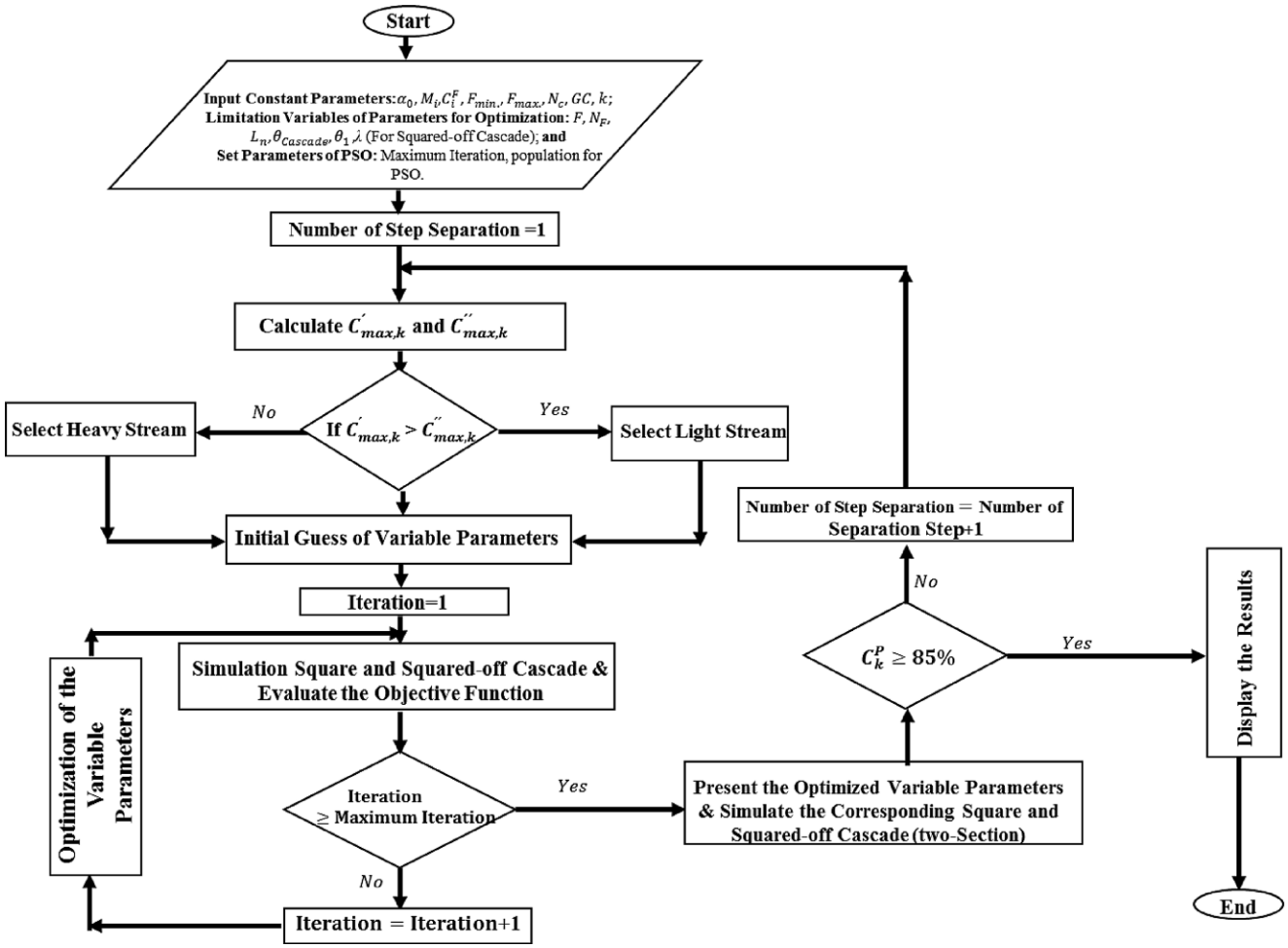

Fig. 5 Procedure of optimization of SC and two-section SOC to achieve the desired enrichment of the target isotope

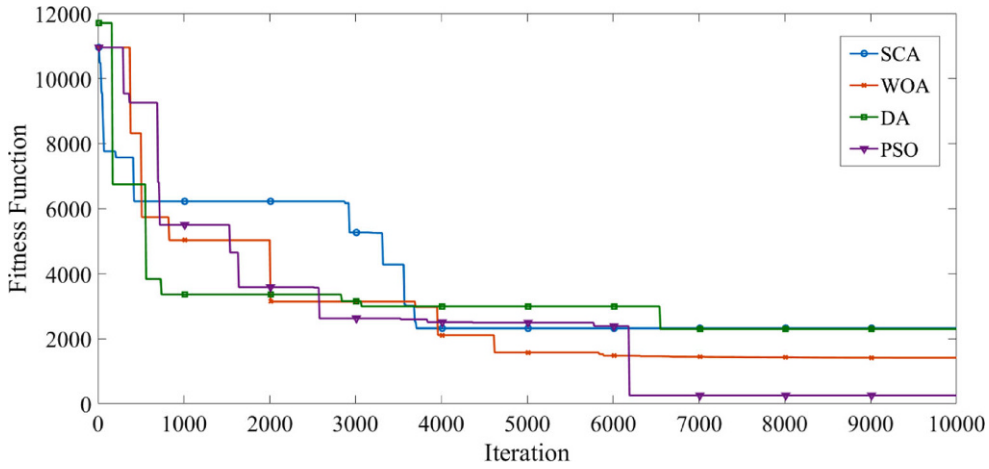

Fig. 6 Fitness function versus iteration numbers for different optimization algorithms

Table 5 The Comparison of the Best Solution for SC Obtained by Different Optimization Algorithms

Optimization Algorithm	ABC [12]	PSO	WOA	SCA	DA
C_{si-28}^{P} (%)	99.9900	99.9900	99.9920	99.9900	99.9910
C_{si-28}^{W} (%)	0.0100	0.0103	0.0088	0.0098	0.0072
N	52	52	52	52	52
N_F	25	8	13	21	18
$\sum L$ (g/s)	291.31	276.12	368.08	550.16	400.76

Optimization results for isotope separation

In this paper, the performance of optimized SC and two-section SOC with a certain number of GCs for the separation of ^{124}Xe from nine stable xenon isotopes up to 85% enrichment is investigated and compared. In order to select the best SC for the enrichment of ^{124}Xe, all possible cascades were examined using 160 GCs, and finally, the best SC was selected. Also, the types of two-section SOC arrangements in proportion to the stage number of the selected SC were investigated. The input parameters for simulation of SC and two-section SOC are presented in Table 6. The overall separation factor per unit molar weight difference (α_0) was considered as a function of the feed flow rate to a single gas centrifuge (Fig. 7).

SC results

The first step in optimizing SCs using the code "SC-PSO" is to determine the number of stages, which is proportional to the number of GCs. The types of states that can form a SC with 160 GCs are presented in Table 7.

In order to achieve 85% enrichment for the ^{124}Xe isotope according to Table 7, the number of stages of SC is considered within the range 8–80 and SC parameters are optimized using the code "SC-PSO." For all of the cases listed in Table 7, more than one separation step is required to increase the ^{124}Xe isotope's enrichment to 85%. Except for a SC with eight stages, the rest of the cascades reached 85% enrichment with three separation steps. It is worth mentioning that increasing the number of separation steps led to a decrease in the overall efficiency. This, in turn, caused the efficiency of the eight-stage cascade to be much lower than that of the other

Table 6 Input Parameters of SC and Two-Section SOC

No	Sign	Values		
1	M_i (g/ mol) & C_i^F (%)	Isotope	M_i (g/ mol)	C_i^F (%)
		^{124}Xe	124	0.09
		^{126}Xe	126	0.09
		^{128}Xe	128	1.92
		^{129}Xe	129	26.44
		^{130}Xe	130	4.08
		^{131}Xe	131	21.18
		^{132}Xe	132	26.89
		^{134}Xe	134	10.44
		^{136}Xe	136	8.87
2	F_{min} (mg/s)	4		
3	F_{max} (mg/s)	20		
4	α_0	$1.20\times F^{-0.05}$		
5	GC	160		

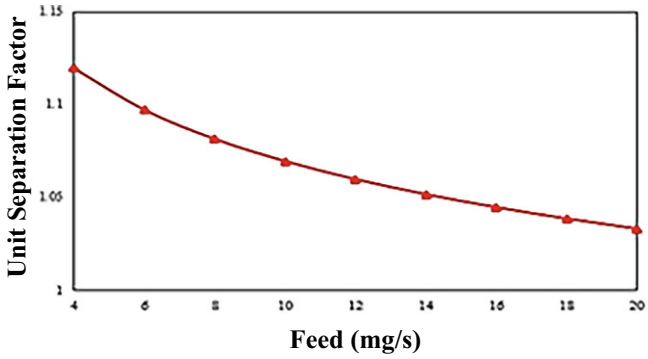

Fig. 7 Dependence of α_0 on the feed flow rate

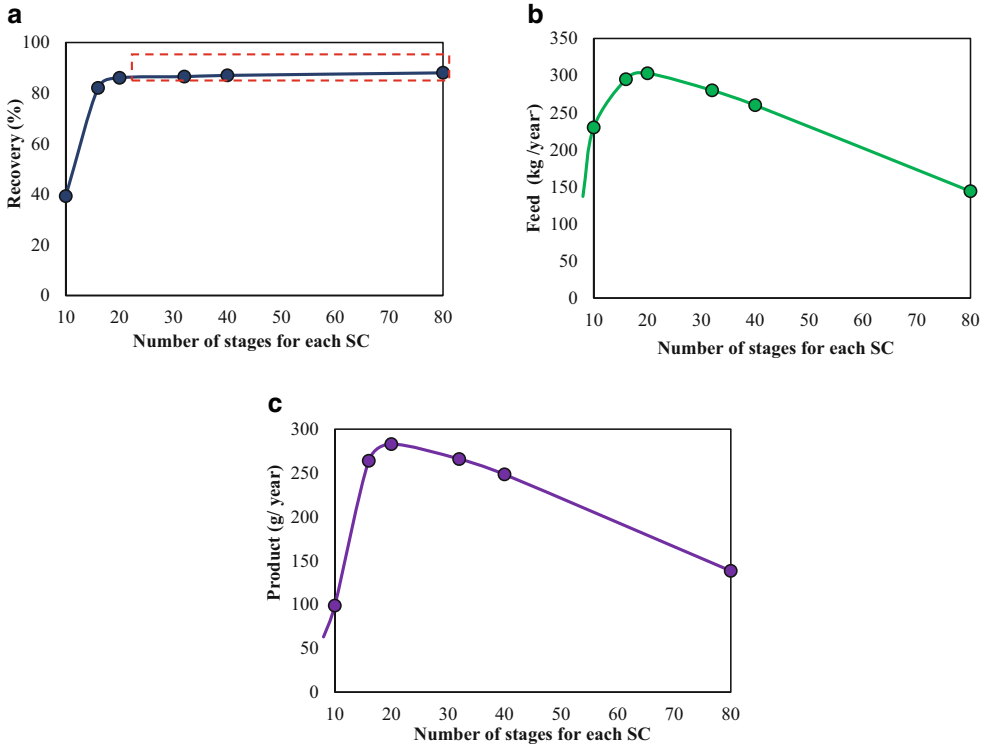

Fig. 8 Trend of changes of (**a**) recovery factor, (**b**) feed consumption, and (**c**) producing product according to the number of stages for the enrichment of ^{124}Xe up to 85% in SC using the code "SC-PSO"

cascades. The results of SCs for different optimizations can be used to determine the most appropriate number of stages (Fig. 8).

According to Fig. 8, by increasing the number of stages, the recovery factor increases, but regarding the stages 20–80, the effect of increasing the number of stages decreases gradually and does not have a significant effect on increasing the recovery factor. On the other hand, increasing the number of stages leads to a decrease in the ease of operation of the cascade and it is better to use cascades with a smaller number of stages. In addition, the amount of product generated in a given period of time is another criterion for selecting the number of stages of an SC; this has been shown in proportion to a period of 1 year in Fig. 8c. As indicated, SC with 20 stages has the highest amount of production compared with other cascades, whereas the value of its recovery factor is slightly different from the 80-stage cascade. Therefore, arrangement number 4, with 20 stages, has been chosen as the best SC arrangement to increase the enrichment of ^{124}Xe. Table 8 presents the results of the optimization of SC (arrangement number 4) using the code "SC-PSO" to increase ^{124}Xe richness from 0.09 to 85% with natural feed over a 1-year period. Figures 9 and 10 show the values of feed flow rate and the light

Table 7 Number of Stages of SCs with 160 GCs

Number of optimization	SC (1)	SC (2)	SC (3)	SC (4)	SC (5)	SC (6)	SC (7)
Number of stages	8	10	16	20	32	40	80
Number of GC	20	16	10	8	5	4	2

Table 8 Characterization of the Optimized SC with 20 Stages for the ^{124}Xe Enrichment Steps

Number of steps	Desired product	Optimized parameters						Cascade specification		
		C_1^P (%)	Feed (mg/s)	N_F	F_{Single} (mg/s)	$\theta_{cascade}$	θ_1	Duration (day)	D	Recovery (%)
1	Light product	1.75	10.520	11	11.995	0.05	0.487	334	0.951	92
2	Light product	33.56	5.999	14	5.661	0.05	0.456	29	0.966	96
3	Light product	85.80	4.040	14	4.000	0.368	0.449	2	0.928	94

Table 9 Results of Optimized SC Using PSO and WOA Algorithms for 20 Stages for ^{124}Xe Isotope Enrichment

No	Type of algorithm	Recovery (%)	Consumed feed (kg/year)	Product (g/year)
1	WOA	78.11	265	219
2	PSO	86.14	303	283

and heavy products of the ^{124}Xe enrichment steps, as well as the concentration distribution of light output flow from the stages. In each stage, there are control valves that are used to operate the cascade and to establish the conditions of SC. Therefore, in order to determine the concentration throughout the cascade, it is necessary to determine the flow rate of feed, light, and heavy products in each stage.

As shown in Fig. 10a, the richness of ^{124}Xe does not increase significantly in the first step. In the second step, the enhancement of the concentration of ^{124}Xe is more considerable and increases to 33.5% (Fig. 10b). Finally, in the last step, the concentration of ^{124}Xe reaches 85% (Fig. 10c).

After determining the optimal SC with the PSO algorithm, the performance of the WOA in SC optimization for the enrichment of the ^{124}Xe isotope up to 85% using 160 GCs and 20 stages was investigated and compared.

It can be concluded from Table 9 that for the separation of the ^{124}Xe isotope, the performance of the algorithms based on the recovery factor, feed capacity, and the amount of production is in the order of PSO> WOA, indicating the greater efficiency of the PSO algorithm in SC optimization.

Table 10 Results of Two-Section SOCs for Various Optimizations Using the Code "SOC-PSO"

Type of arrangement	Number of the arrangement	Arrangement (GC* Stage)		Consumption feed (kg/year)	Produced (g/year)	Recovery factor (%)
		Section 1	Section 2			
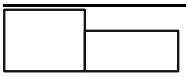	1	**15 × 9**	**5 × 5**	306	318	**92.84**
	2	**16 × 9**	**4 × 4**	306	315	92.55
	3	**10 × 10**	**10 × 6**	273	281	92.00
	4	**10 × 9**	**10 × 7**	255	262	91.85
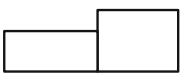	5	**10 × 7**	**10 × 9**	219	222	90.90
	6	**10 × 6**	**10 × 10**	179	177	89.01
	7	**12 × 6**	**8 × 11**	320	317	88.52
	8	**14 × 5**	**6 × 15**	288	285	88.49

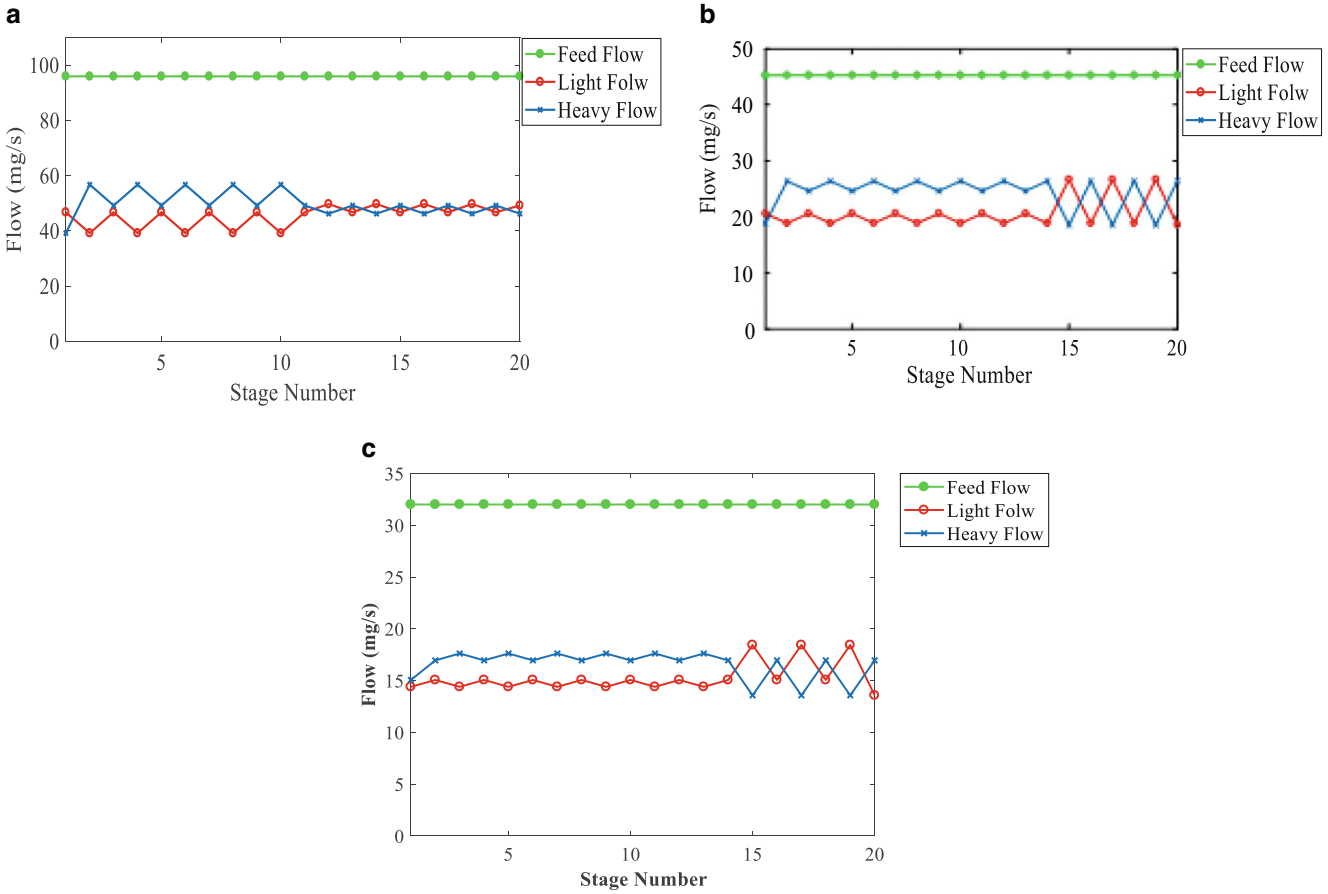

Fig. 9 The feed, light, and heavy flow rates of different stages in a square cascade for the enrichment of ^{124}Xe: (**a**) first step, (**b**) second step, (**c**) third step

Results of two-section SOC

Similar to SC optimization, the first step in the design of two-section SOCs is to determine the number of stages and the arrangement of the cascades. As SC with 20 stages is the most suitable cascade for the enrichment of ^{124}Xe, there are considered to be 20 SOC stages. In order to determine the arrangement of two-section SOC, it is necessary to first determine whether feed enters the first or the second section. For this purpose, different arrangements in which the feed enters the first or second sections were investigated (Table 10). Table 11 presents the results of optimizing two-section SOCs for the enrichment of ^{124}Xe up to 85% using the code "SOC-PSO" over a 1-year period. As shown, for all states of two-section SOCs, the recovery factor of ^{124}Xe is higher than that of the selected SC, which indicates the better performance of SC. Among the two-section SOCs, the cascades

Table 11 Characterization of Optimized Two-Section SOC for Number One Arrangement

Number of steps	Desired product	Optimized parameters						Cascade specification		
		Feed (mg/s)	C_1^P (%)	N_F	$\theta_{cascade}$	θ_1	λ	Duration (day)	D	Recovery (%)
1	Light product	10.520	1.16	14	0.080	0.391	0.532	298	0.921	98
2	Light product	5.999	11.31	14	0.101	0.397	0.256	38	0.910	98.01
3	Light product	4.040	85.00	11	0.129	0.499	0.406	29	0.977	96.66

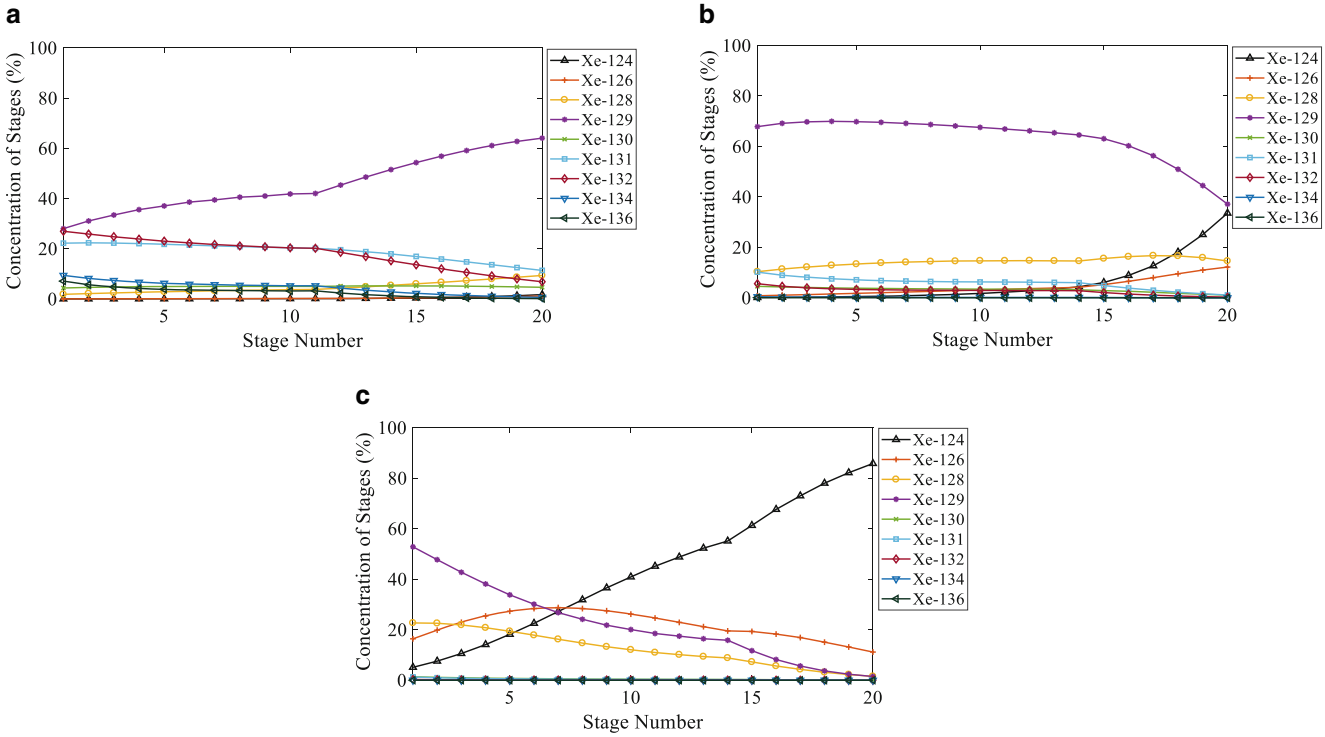

Fig. 10 Concentration distribution of the light streams of all stages in a square cascade for the enrichment of ^{124}Xe: (**a**) first step, (**b**) second step, (**c**) third step

whose feed enters the first section have greater efficiency in the enrichment of ^{124}Xe. Among the types of SOCs, the arrangement of number one has the best performance in efficiency and product generation during a period of 1 year. The characteristics of the optimal two-section SOC (the arrangement of number one) for all steps are given in Table 11. The feed and light and heavy flow rates of the stages are presented in Fig. 11. In order to determine the concentration throughout the cascade, it is necessary to determine the flow rate of feed, light, and heavy products in each stage. Figure 12 shows the concentration distribution of the light streams of all stages. As can be seen in Fig. 12a, the concentration of ^{124}Xe does not increase much in the first step. In the second step, the increment of concentration of ^{124}Xe is more noticeable and increases to 11.31% (Fig. 12b). Finally, in the third step, the concentration of ^{124}Xe reaches 85% (Fig. 12c).

After determining the optimal arrangement of two-section SOCs using the PSO algorithm, the performance of the WOA in the optimization of two-section SOC for the enrichment of ^{124}Xe up to 85% using 160 GCs under the same conditions was compared.

The values presented in Table 12 show that the PSO algorithm has performs better in the two-section SOC optimization for the separation of ^{124}Xe isotope compared with the WOA. It is worth noting that the superiority of the PSO algorithm over the other algorithm cannot be attributed to all problems; according to the no-free lunch theory, depending on the specific physics of the problem and compatibility with the problem structure, only one specific algorithm can work well in this regard [21].

Table 12 Results of Optimized Two-Section SOCs with PSO and WOA Algorithms for Arrangement No. 1 for the Enrichment of ^{124}Xe Isotope

No	Type of algorithm	Recovery (%)	Consumed feed (kg/year)	Product (g/year)
1	WOA	83.41	280	249
2	PSO	92.84	306	318

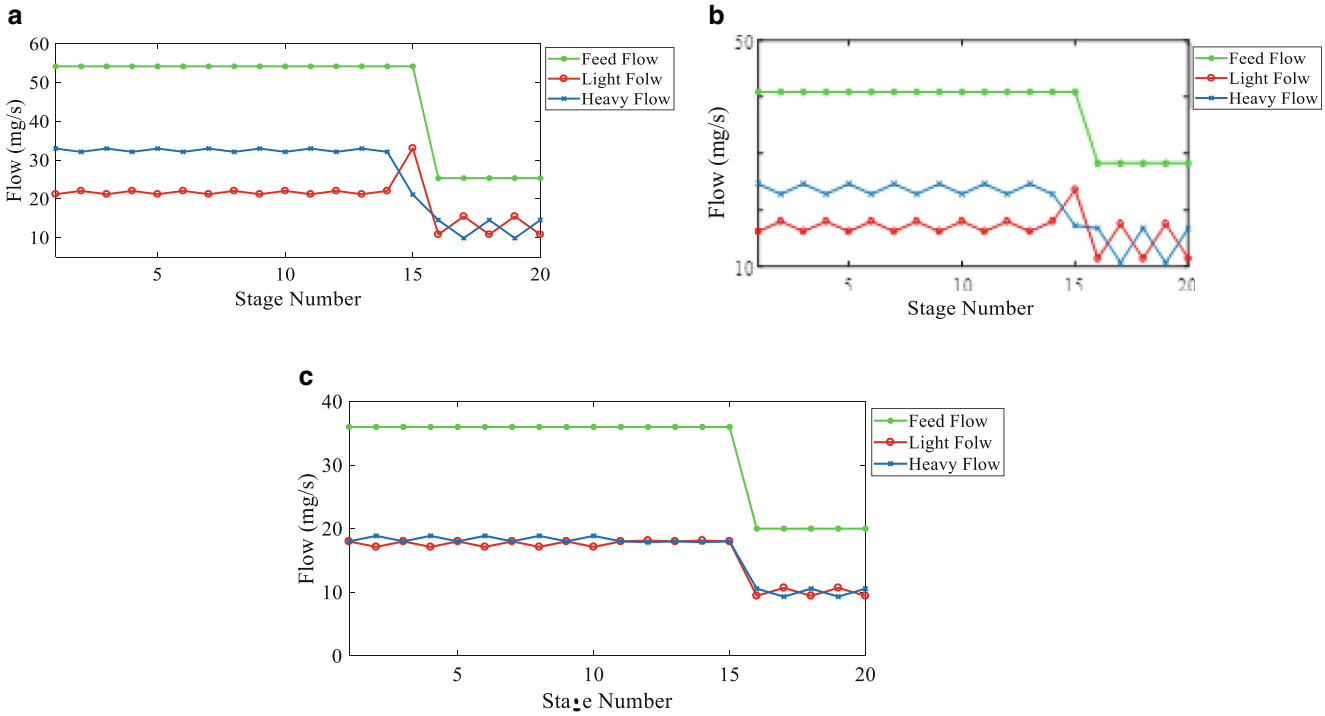

Fig. 11 The feed, light, and heavy flow rates of different stages in two-section SOC for the enrichment of ^{124}Xe: (**a**) first step, (**b**) second step, (**c**) third step

As a result, the recovery factor of the best SC and two-section SOC consisting of 20 stages is 86.14% and 92.84% respectively. Also, the amount of product obtained by the best SC and two-section SOC is 283 (g/year) and 318 (g/year) respectively. As expected, under the same conditions, the amount of product and the recovery factor of SOC are higher than for SC, which indicates the superior performance of SOCs.

Conclusions

In this study, the optimized SC and two-section SOC with 160 GCs to enrich the ^{124}Xe isotopes up to 85% from a combination of nine components of stable isotopes of the xenon element are proposed separately using the codes "SC-PSO," "SC-WOA," "SOC-PSO," and "SOC-WOA." PSO and the WOA were used to optimize the cascade parameters. All possible SCs were examined with 160 GCs for the enrichment of ^{124}Xe using "SC-PSO." Finally, it was found that the recovery factor increases by increasing the number of stages nonlinearly. On the other hand, in a SC with 20 stages, the amount of product reached its maximum during a specified period of time. Owing to the little difference in the recovery factor between this cascade and the longer cascades, it was selected as the most suitable SC to increase the enrichment of ^{124}Xe. Then all cases of two-section SOCs with 20 stages in which the feed enters the first or second part were examined using "SOC-PSO." The results showed that the SOCs in which the feed enters the first section perform better with regard to the enrichment of ^{124}Xe. Finally, the most suitable two-section SOC, where the first section consisted of 15 stages with nine gas centrifuges and the second section consisted of five stages with five gas centrifuges, was selected for the enrichment of ^{124}Xe using "SOC-PSO." Also, the performance of PSO and the WOA was compared based on the recovery factor, feed capacity, and amount of production for SC and SOC. The recovery coefficient of the ^{124}Xe isotope by the codes "SC-PSO," "SC-WOA," "SOC-PSO," and "SOC-WOA" was obtained as 86.14, 74.30, 92.84, and 83.41% respectively. It was revealed that, compared with the WOA, the PSO algorithm has greater

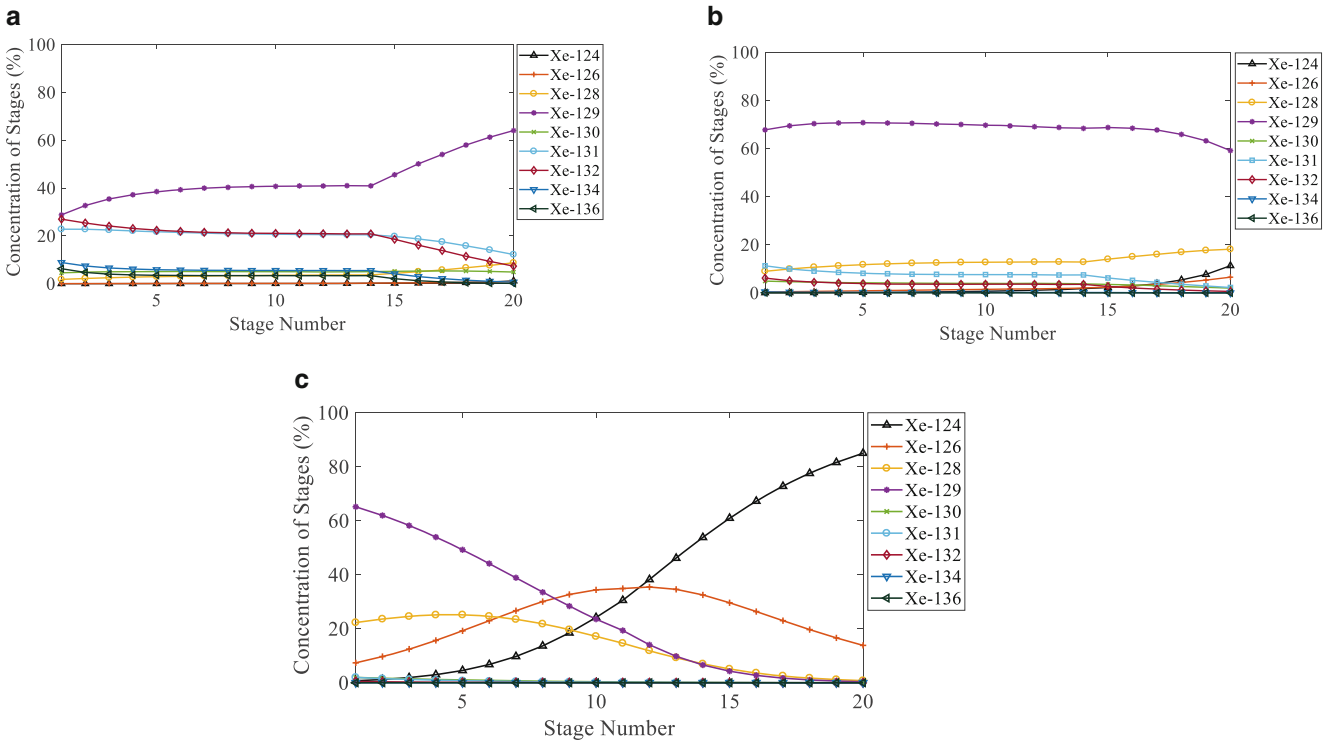

Fig. 12 Concentration distribution of the light streams of all stages in two-section SOC for the enrichment of ^{124}Xe: (**a**) first step, (**b**) second step, (**c**) third step

the algorithm's compatibility with the problem structure, according to the no-free lunch theory. In addition, under the same conditions, the amount of product and the recovery factor of SOC are higher than those of SC, which indicates the superior performance of SOCs.

Nomenclature

The nomenclature is shown in Table 13.

Table 13 Nomenclature

		Unit
Nomenclature		
n	Number of stages	(–)
M	Molecular weight	(mg/s)
N	Total number of stages in a cascade	(–)
N_1	Total number of stages in the first section	(–)
N_2	Total number of stages in the second section	(–)
N_F	Feed position in the cascade	(–)
$F_{\min}$	Minimum feed flow rate of a single machine	(mg/s)
F_{Single}	Feed flow rate of a single machine	(mg/s)
$F_{\max}$	Maximum feed flow rate of a single machine	(mg/s)
F	Feed flow rate of a cascade	(mg/s)
C_i^F	Isotope concentration in the cascade feed stream	(–)

Table 13 (Continued)

		Unit
P or L	Final light stream of a cascade	(mg/s)
W or H	Final heavy stream of a cascade	(mg/s)
L_n	Stage feed stream	(mg/s)
$L\prime_n$	Light stream	(mg/s)
$L\prime\prime_n$	Heavy stream	(mg/s)
C_k^P	Concentration of the desired isotope in the final product stream	(–)
$C\prime_{i,n}$	Concentration of the desired isotope in the light stream	(–)
$C\prime\prime_{i,n}$	Concentration of the desired isotope in the heavy stream	(–)
$C_{i,n}$	Concentration of the desired isotope in the stage feed stream	(–)
Greek Symbols		
α_0	Overall separation factor (per unit molecular weight difference)	(–)
Θ_n	Stage cut with number n	(–)
θ_1	First stage cut	(–)
θ_{Cas}	Cascade cut	(–)
ε_1	Return flow of the first stage	(mg/s)
$\varepsilon\prime_N$	Return flow of the last stage	(mg/s)
λ	Return flow fraction between the first and second sections	(–)

References

1. Ezazi, F., Mallah, M.H., Sabet, J.K., Norouzi, A., Mahmoudian, A.: Investigation on the net cascade using ant colony optimization algorithm. Prog. Nucl. Energy. **119**, 103169 (2020)
2. Wafelman, A., Konings, M.: Synthesis, radiolabeling and stability of radioiodinated m-iodobenzylguanidine, a review. Appl. Radiat. Isot. **45**, 997–1007 (1994)
3. Khooshechin, S., Mansourzadeh, F., Imani, M., Safdari, J., Mallah, M.H.: Optimization of flexible square cascade for high separation of stable isotopes using enhanced PSO algorithm. Prog. Nucl. Energy. **140**, 103922 (2021)
4. Villani, S.: Enrichment of uranium, 1st edn. Springer, Berlin (1979)
5. Benedict, M., Pigford, T.H., Wolfganglevi, H.: Nuclear chemical engineering. McGraw-Will book Co, New York
6. Ying, C., Von Halle, E., Wood, H.G.: The optimization of squared-off cascades for isotope separation. Nucl Technol **105**, 184–189 (1994)
7. Aisen, E.M., Borisevich, V.D., Potapov, V.D., Rudnev, I.A., Sulaberidze, G.A., Tikhomirov, A.V.: Computing experiments for study of cadmium isotope separation by gas centrifuges. Nucl. Instrum. Methods. Phys. Res. B. **417**, 428–433 (1998)
8. Kholpanov, L.P., Potapov, D.V., Sulaberidze, G.A., Chuzhinov, V.A.: On the calculation of a squared-off cascade for multicomponent isotope separation. Chem. Eng. Process. **37**, 359–365 (1998)
9. Borisevich, V., Litvin, Y.V., Sulaberidze, G.A.: Calculational study of the enrichment of cadmium isotopes in gas centrifuges. Theor. Found. Chem. Eng. **41**, 851–858 (2007)
10. Borisevich, V., Yan, J., Smirnov, A.Y., Bonarev, A.K., Zeng, S., Sulaberidze, G.A., Jiang, D.: Cascade design for isotopically modified molybdenum as an alternative to zirconium alloys. Chem. Eng. Res. Des. **218**, 257–264 (2017)
11. Mansourzadeh, F., Safdari, J., Norouzi Khamesh, A., Khajenouri, M.: Comparison of optimum tapered cascade and optimal square cascade for separation of xenon isotopes using enhanced TLBO algorithm. Sep. Sci.tech. **53**, 2074–2087 (2018)
12. Azizov, T.E., Smirnov, A.Y., Sulaberidze, G.A.: Optimization of a square cascade of centrifuges for separation of multicomponent mixtures of stable isotopes. At. Energy. **128**, 291–296 (2020)
13. Zeng, S., Ying, C.: A robust and efficient calculation procedure for determining concentration distribution of Multicomponent mixtures. Sep. Sci. Tech. **35**, 613–622 (2000)
14. Sulaberidze, G.A., Borisevich, V.D.: Cascade for separation of multicomponent isotope mixtures. Sep. Sci. Tech. **36**, 8–9 (2001)
15. Zeng, S., Chuntong, Y.: A method of separating a middle component in multicomponent isotope mixtures by gas centrifuge cascades. Sep. Sci. Tech. **35**, 2173–2186 (2000)
16. Ezazi, F., Mallah, M.H., Safdari, J., Mirmohammadi, S.L.: Performance comparison of the optimized k-section squared-off cascades for enrichment of 124Te using two meta-heuristic paradigms. Prog. Nucl. Energy **145**, 104105 (2022)

17. Imani, M., Keshtkar, A.R., Rashidi, A., Karimi Sabet, J., Noroozi, A.: Investigation on the effect of holdup and cascade shape in NFSW cascades. Prog. Nucl. Energy. **119**, 103182 (2020)
18. Naserbegi, A., Aghaie, M.: Multi-objective optimization of hybrid nuclear power plant coupled with multiple effect distillation using gravitational search algorithm based on artificial neural network. Therm. Sci. Eng. Prog. **19**, (2020)
19. Robinson, J., Sinton, S., Rahmat-Samii, Y.: Particle swarm, genetic algorithm, and their hybrids: optimization of a profiled corrugated horn antenna. In: IEEE, antennas and propagation society international symposium and URSI national radio science meeting, vol. 7467812. San Antonio (2002)
20. Mirjalili, S.A., Lewis, A.: The whale optimization algorithm. Adv. Eng. Softw. **95**, 51–67 (2016)
21. Wolpert, D.H., William, G.M.: No free lunch theorems for optimization. ieee. Trans. Evol. Comput. **1**, (1997)

Authors and Affiliations

✉ Fatemeh Ardestani
Fatemehardestani66@yahoo.com

Jaber Safdari

Mohammad Hassan Mallah

Morteza Imani

Fatemeh Ardestani, Jaber Safdari, Mohammad Hassan Mallah, Morteza Imani
Materials and Nuclear Fuel Research School, Nuclear Science and Technology Research Institute, Tehran, Iran